Supplementary Material

Supplementary method and materials

Text S1:

To facilitate the experiments, the grain size number percentages must be converted to mass fractions, after which turbidity-SSC curves can be prepared by mixing suspensions according to the grain size distribution proportions of the suspended sediment samples.

From $m = \rho V$, assuming that particle density ρ is constant across the small catchment, therefore,

$$\frac{m_1}{m_2} = \frac{V_1}{V_2} = \frac{{}^4/_3\,\pi(\frac{d_1}{2})^3}{{}^4/_3\,\pi(\frac{d_2}{2})^3} = \frac{d_1^3}{d_2^3} \tag{S1}$$

For example, when d_1=50μm and d_2=63μm, the mass ratio of two individual particles is m_1/m_2: $50^3/63^3$=125000/250047≈1/2.

If their number proportions in the same sample are N_1/N_2: 1.017%/3.058%, then the corresponding mass ratio is M_1/M_2: 1.017%×1/3.058%×2=1/6.014.

Text S2:

(1) Coefficient of determination (R^2) can be calculated as follows:

$$R^2 = \frac{\left[\sum_{i=1}^{n}(Q_{0,i} - \overline{Q}_0)(Q_{m,i} - \overline{Q}_m)\right]^2}{\sum_{i=1}^{n}(Q_{0,i} - \overline{Q}_0)^2 \sum_{i=1}^{n}(Q_{m,i} - \overline{Q}_m)^2} \tag{S2}$$

where $\bar{Q}_0$ is the mean of the observed values, and $\bar{Q}_m$ is the mean of the simulated values. The R^2 value ranges from 0 to 1. The closer R^2 is to 1, the better the match between the simulated and observed values, indicating better model performance.

(2) Nash–Sutcliffe efficiency (NSE) coefficient can be calculated as follows:

$$NSE = 1 - \frac{\sum_{i=1}^{n}(Q_{0,i} - Q_{m,i})^2}{\sum_{i=1}^{n}(Q_{0,i} - \overline{Q}_0)^2} \tag{S3}$$

Notably, the NSE value ranges from 0 to 1. The closer the NSE value is to 1, the better the agreement between the simulated and observed values, indicating better model performance.

(3) Root mean square error (RMSE) can be calculated as follows:

$$\mathrm{RMSE} = \sqrt{\sum_{i=1}^{n} \frac{(\hat{y}_i - y_i)^2}{n}} \tag{S4}$$

where n is the number of samples, y_i denotes the observed value, and $\hat{y}_i$ denotes the predicted value. The unit of RMSE is the same as that of the predicted variable, and a smaller RMSE indicates higher predictive accuracy of the model.

Text S3:

Using suspended sediment grain size composition percentages from the fitting segment of the spring snowmelt period at the glacier terminus, this study fitted a set of power law functions to construct a function group that describes how the proportion of each grain size fraction varies with turbidity across this range:

$$\begin{cases} y_1 = 0.4465 \cdot T^{0.4204}, & 50\mu m \le d \le 75\mu m \\ y_2 = 0.4197 \cdot T^{0.3468}, & 75\mu m < d \le 125\mu m \\ y_3 = 0.4872 \cdot T^{0.3119}, & 125\mu m < d \le 250\mu m \\ y_4 = 0.0169 \cdot T^{0.5552}, & 250\mu m < d \le 320\mu m \\ y_5 = 0.2408 \cdot T^{0.1216}, & 320\mu m < d \le 500\mu m \\ y_6 = 1.4405 \cdot T^{0.0528}, & 500\mu m < d \le 900\mu m \\ y_7 = 0.4714 \cdot T^{0.0911}, & 900\mu m < d \le 1250\mu m \\ y_8 = 100\% - \sum_{n=1}^{n=7} y_i\,, & 0.5\mu m \le d < 50\mu m \end{cases} \tag{S5}$$

Supplementary Table

Table S1. Parameters of the power-law regression equations for turbidity–SSC relationships derived from laboratory mixing experiments and field monitoring.

Different Cross-Sections Different Periods	Coefficient *a* of the regression equation reproduced by the laboratory mixing experiments	Coefficient *a* of the regression equation derived from field monitoring	Exponent *b* of the regression equation reproduced by the laboratory mixing experiments	Exponent *b* of the regression equation derived from field monitoring
Glacier terminus section Snowmelt period	0.0017	0.0021	1.1734	1.1480
Glacier terminus section Glacier melt period	0.0033	0.0032	1.1846	1.1842
Glacier terminus section Rainfall dominated period	0.0013	0.0017	1.1832	1.1229
Basin outlet section Snowmelt period	0.0012	0.0007	1.1318	1.2873
Basin outlet section Glacier melt period	0.0023	0.0024	1.0734	1.0699
Basin outlet section Rainfall dominated period	0.0014	0.0020	1.0888	1.1531

Supplementary Figures

Fig. S1. Runoff and sediment conditions in the Kuoqionggangri Glacier Basin during different periods.

Note: (a) snowmelt period, (b) glacier melt period, and (c) rainfall period.

目数	孔径（mm）	目数	孔径（mm）	目数	孔径（mm）
2目	12.5	45目	0.4	220目	0.065
3目	8	50目	0.355	240目	0.063
4目	6	55目	0.315	250目	0.061
5目	5	60目	0.28	280目	0.055
6目	4	65目	0.25	300目	0.050
8目	3	70目	0.224	320目	0.045
10目	2	75目	0.2	325目	0.043
12目	1.6	80目	0.18	340目	0.041
14目	1.43	90目	0.16	360目	0.040
16目	1.25	100目	0.154	400目	0.0385
18目	1	110目	0.15	500目	0.0308
20目	0.9	120目	0.125	600目	0.026
24目	0.8	130目	0.112	800目	0.022
26目	0.71	140目	0.105	900目	0.020
28目	0.68	150目	0.100	1000目	0.015
30目	0.6	160目	0. 096	1800目	0.010
32目	0.58	180目	0. 09	2000目	0.008
35目	0.50	190目	0. 08	2300目	0.005
40目	0.45	200目	0.074	2800目	0.003

Fig. S2. Sieving and weighing of source area soils and suspended sediment samples.

Fig. S3. Experimental procedures and equipment used.

Note: (a) soil sieving, (b) mixing during the experiments, (c) sensor, mixer, and container, (d) power supply box, (e) turbidity meter main unit, and (f) laptop data receiver.

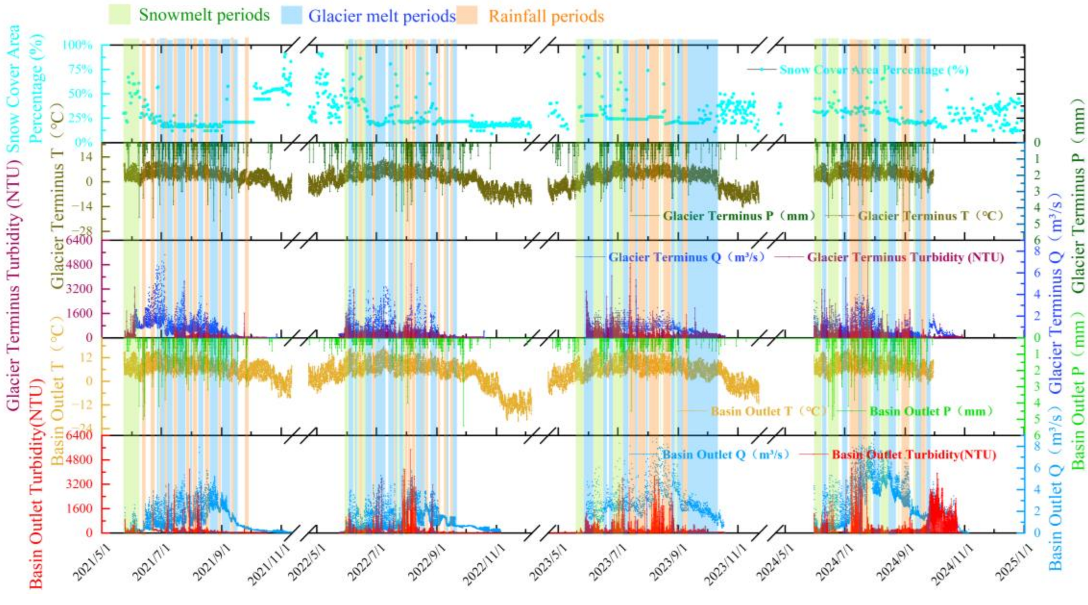

Fig. S4. Monitoring results for the air temperature (T), precipitation (P), discharge (Q) and Turbidity along with remote sensing snow cover area marked with the snowmelt, glacier melt, and rainfall-dominated periods during 2021–2024.

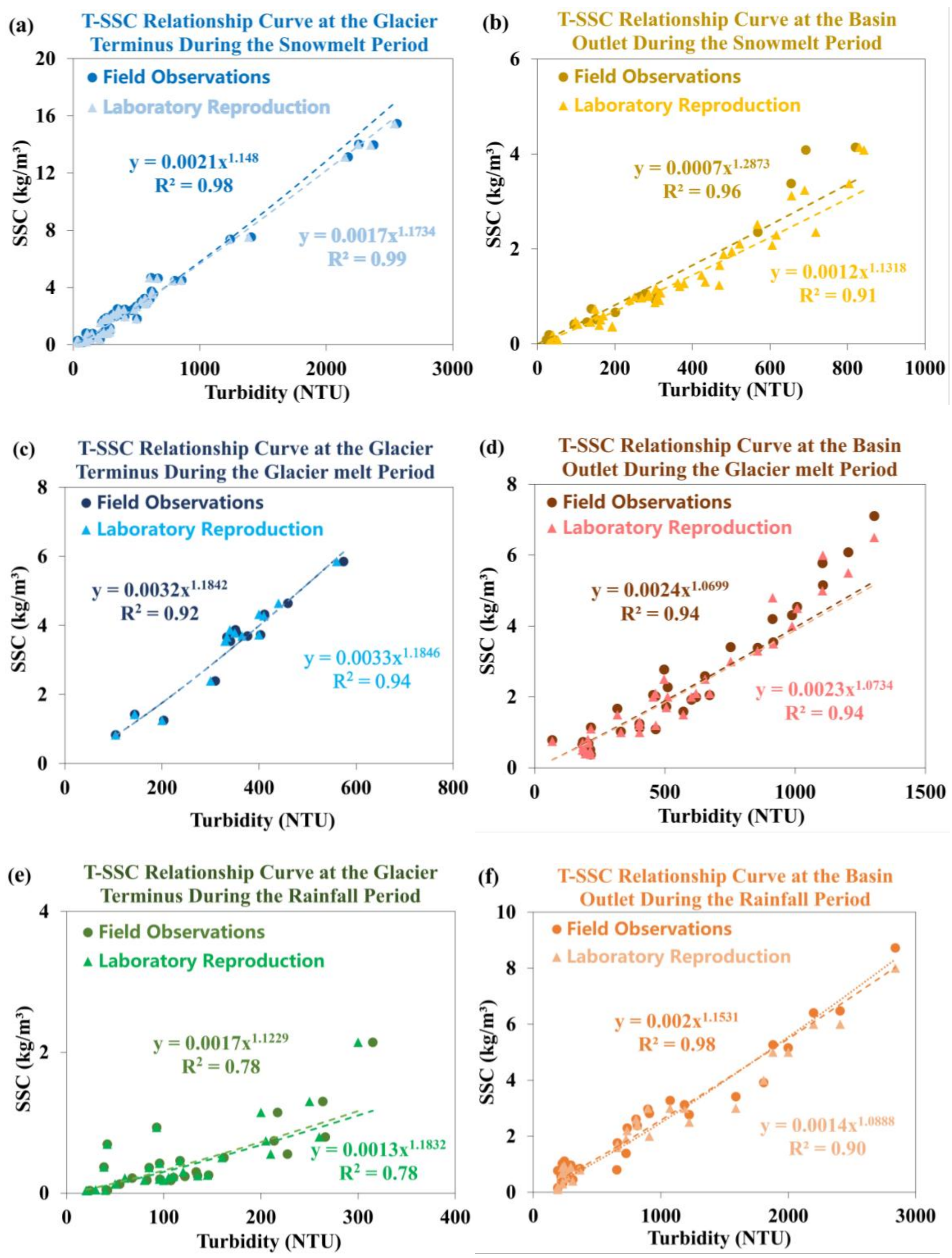

Fig. S5. Laboratory mixing experiments reproducing the field-observed turbidity–SSC relationship curve at the glacier terminus during the snowmelt period (a), the glacier melt period (c), the rainfall period (e); at the basin outlet during the snowmelt period (b), the glacier melt period (d), the rainfall period (f).

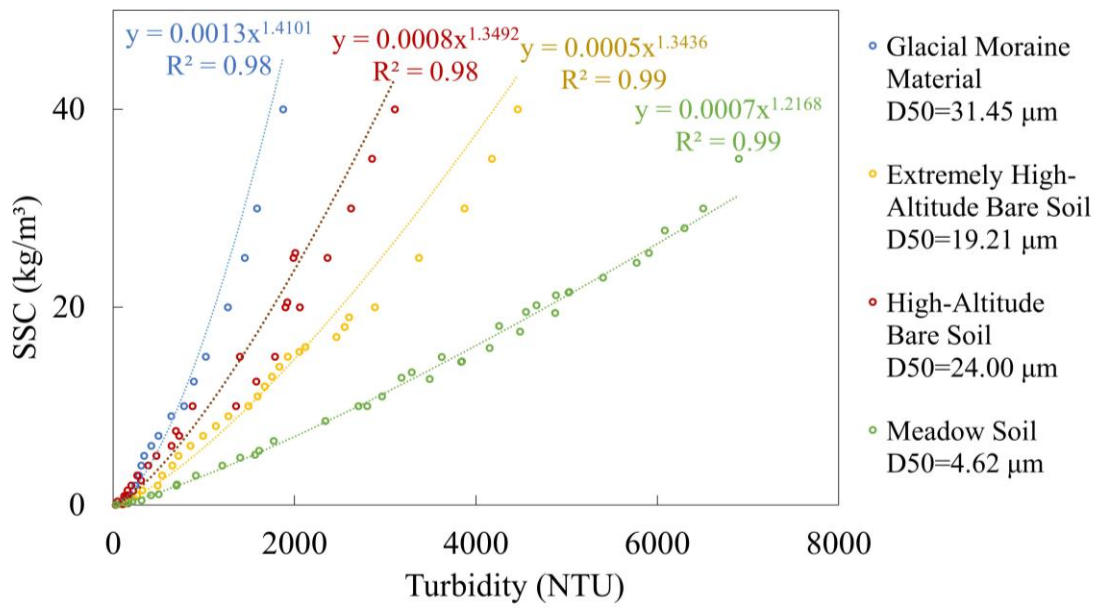

Fig. S6. Turbidity-SSC curves for single sediment sources with different median grain sizes.

Note: D50 denotes the grain size on the cumulative distribution curve at which 50% of the mass (or volume) is finer. It is widely used as a summary metric of soil or sediment texture, although other indices such as D10, D90, mean grain size, skewness, and kurtosis can also capture additional aspects of grain size characteristics.

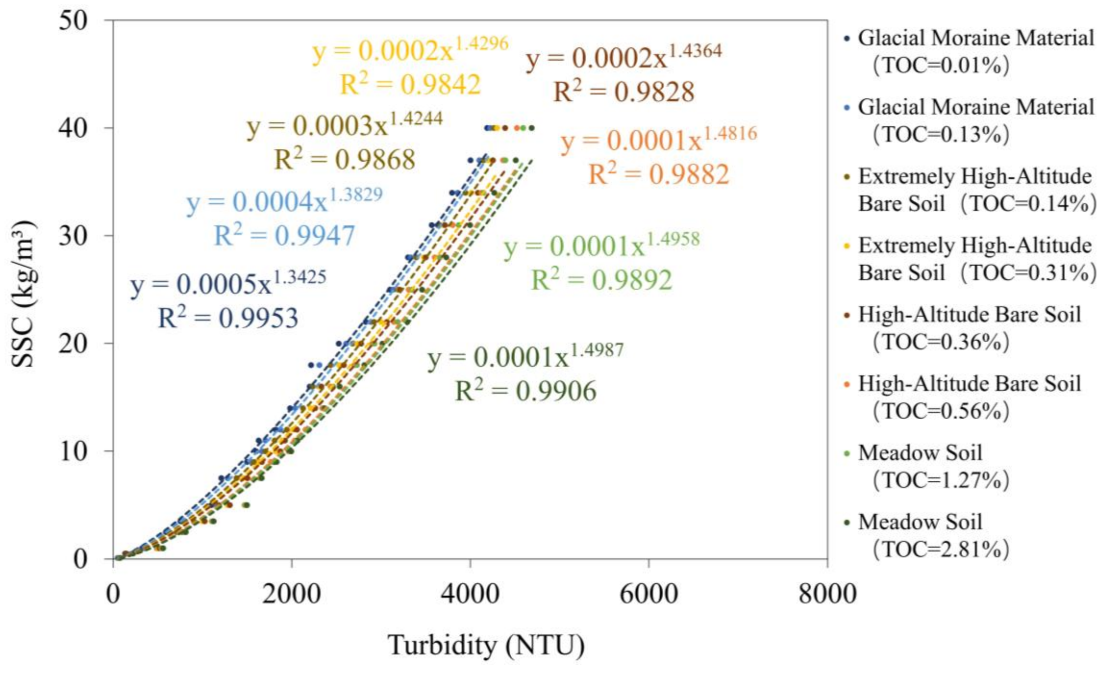

Fig. S7. Turbidity-SSC relationships under different organic matter contents.

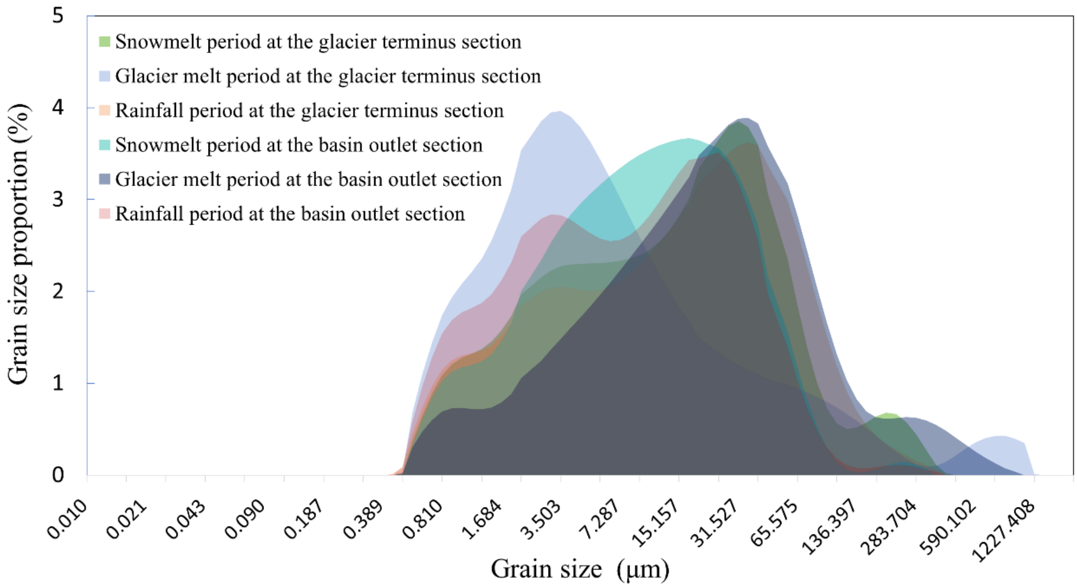

Fig. S8. Grain size composition proportions of suspended sediment under different dominant regimes.

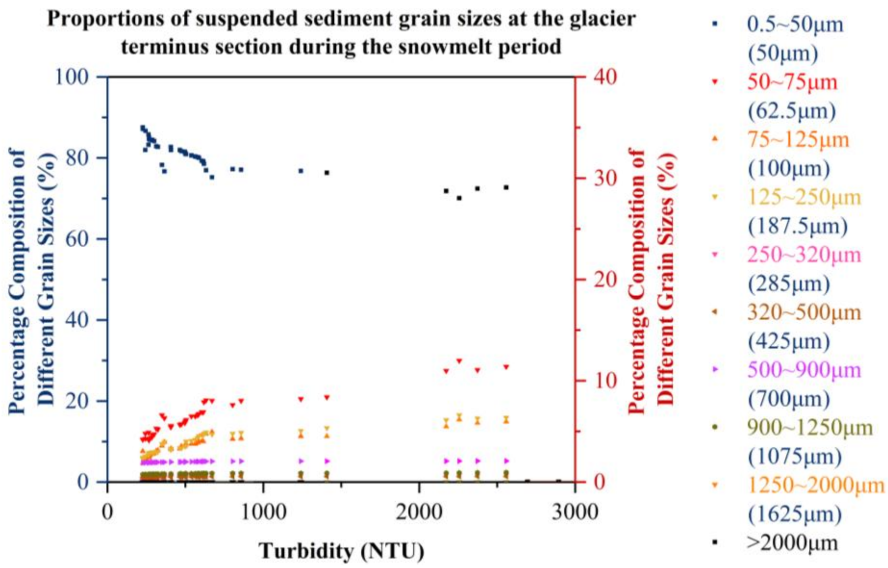

Fig. S9. Percentage composition of suspended sediment grain-size fractions.

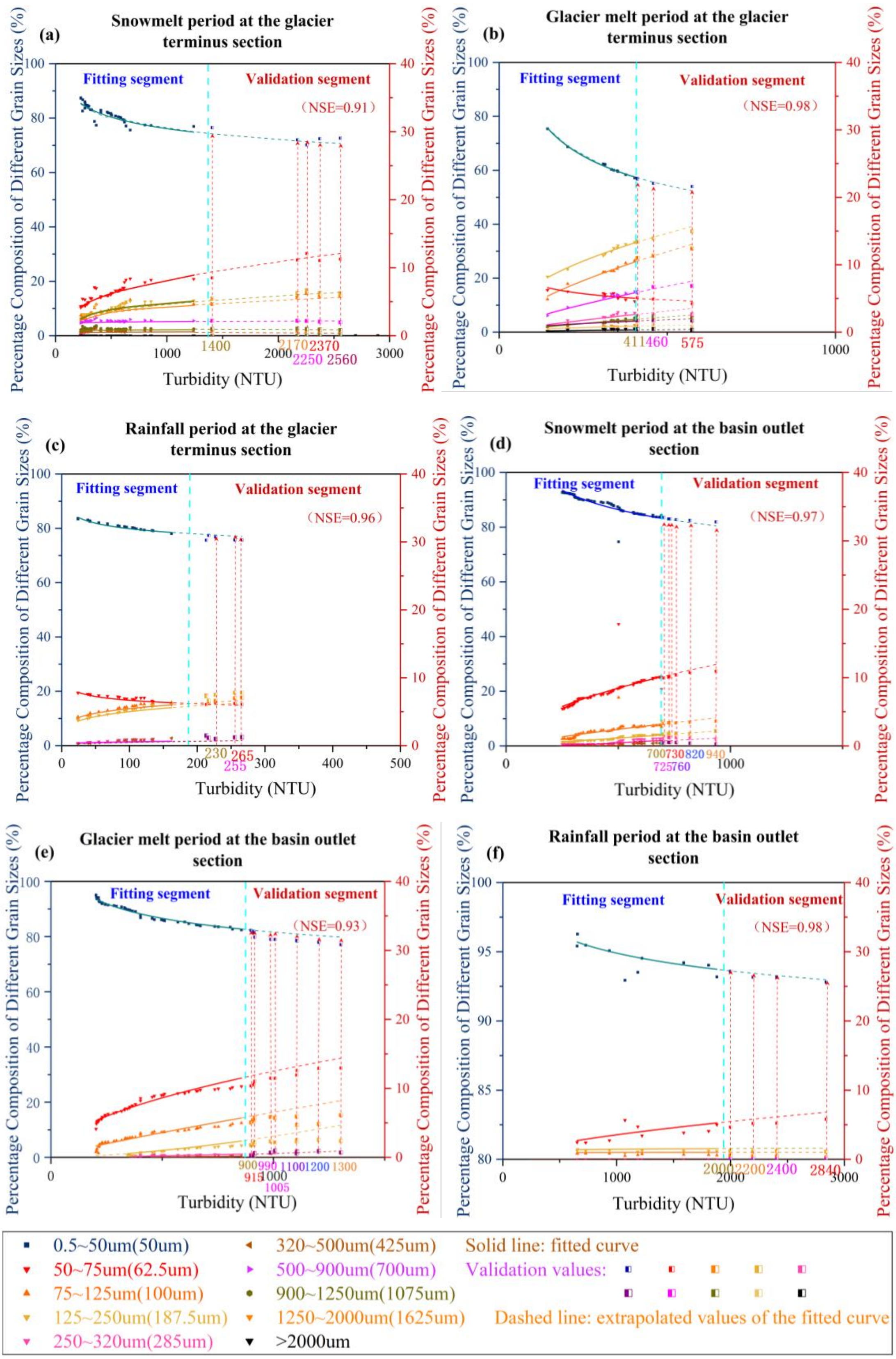

Fig. S10. Validation results for extending the trends in suspended sediment grain size percentage composition.

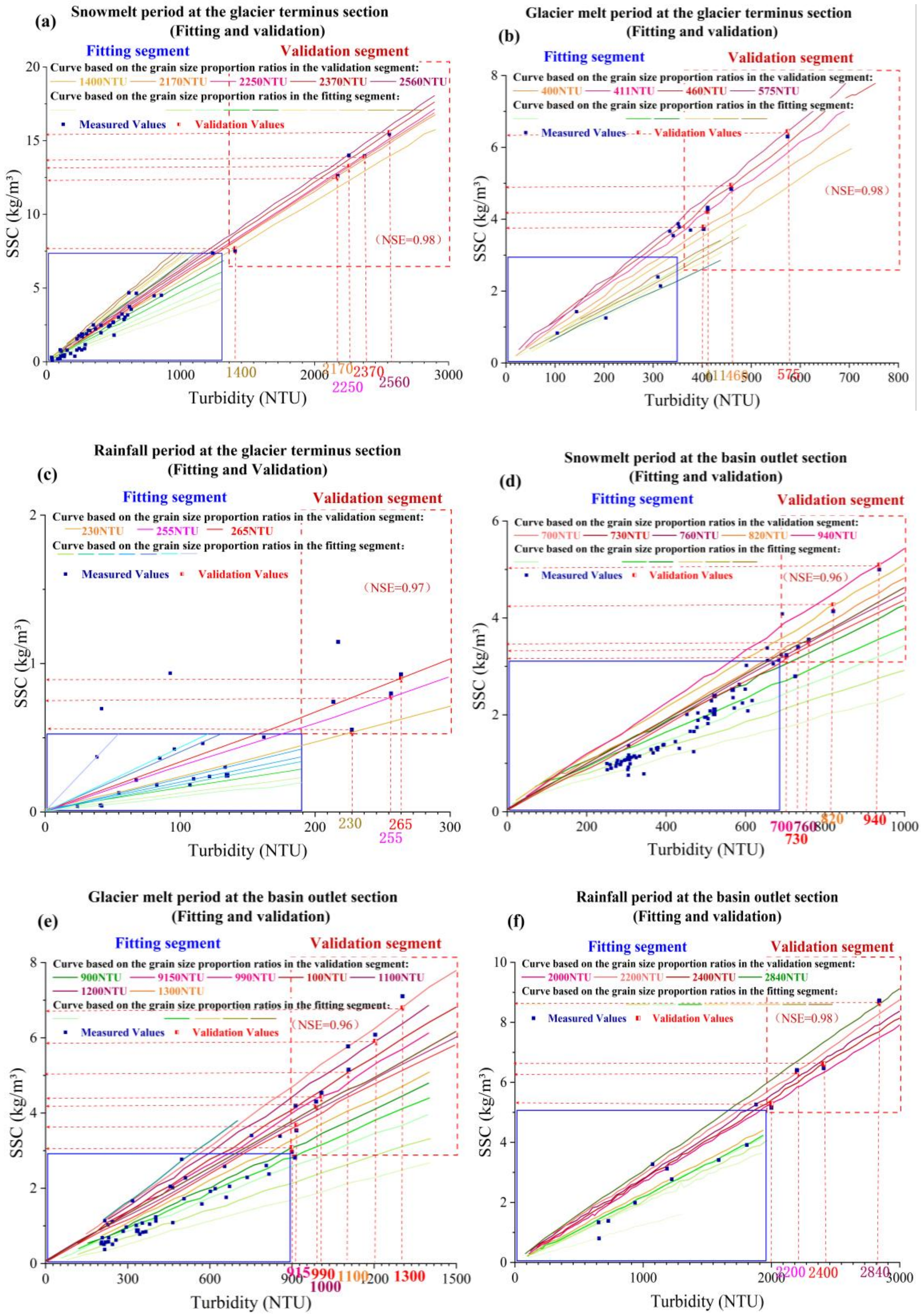

Fig. S11. Validation results for extending the trends in suspended sediment grain size percentage composition.

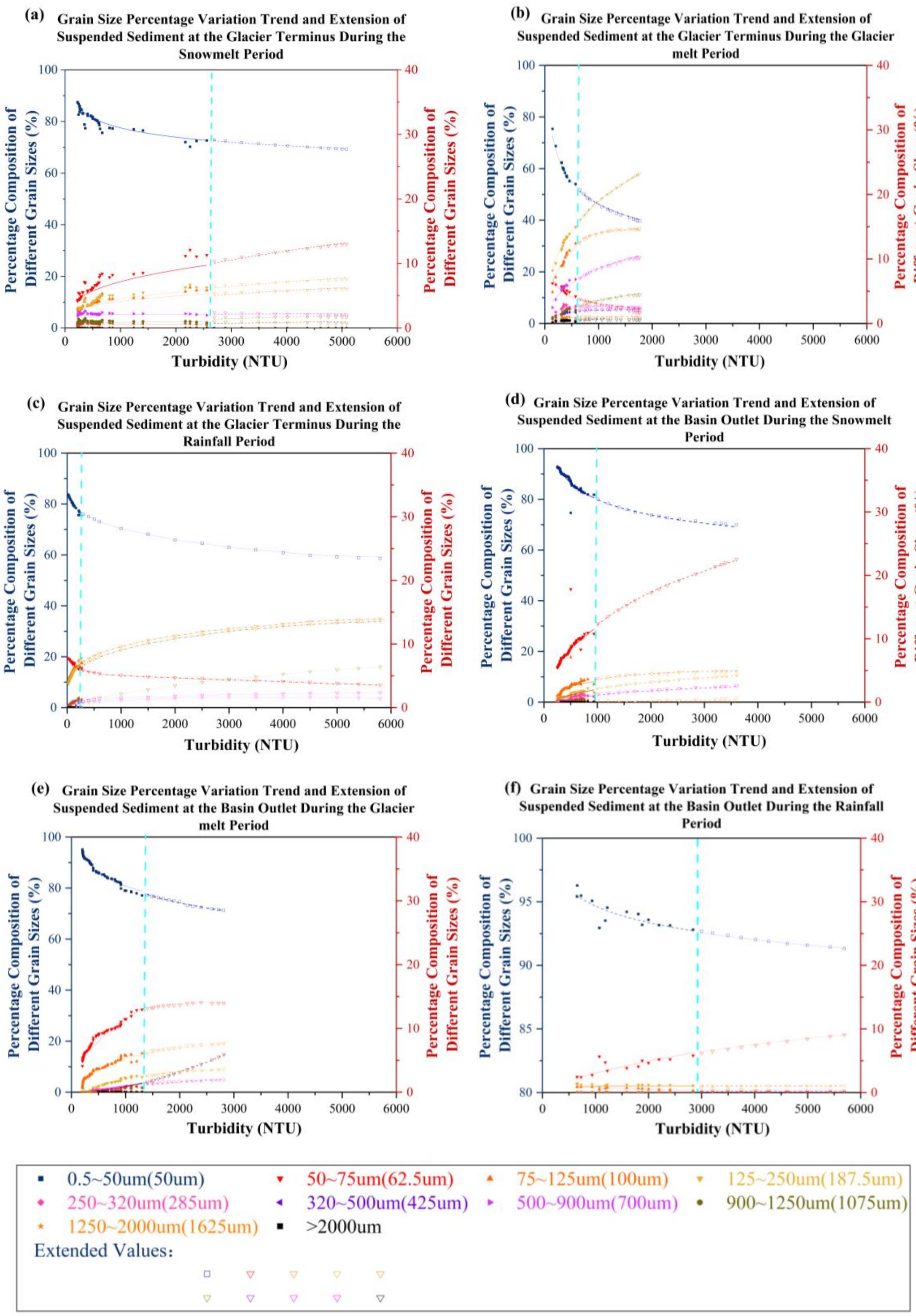

Fig. S12. Results of the extended grain size composition proportions.

Note: filled symbols represent measured values, and open symbols represent extrapolated values.

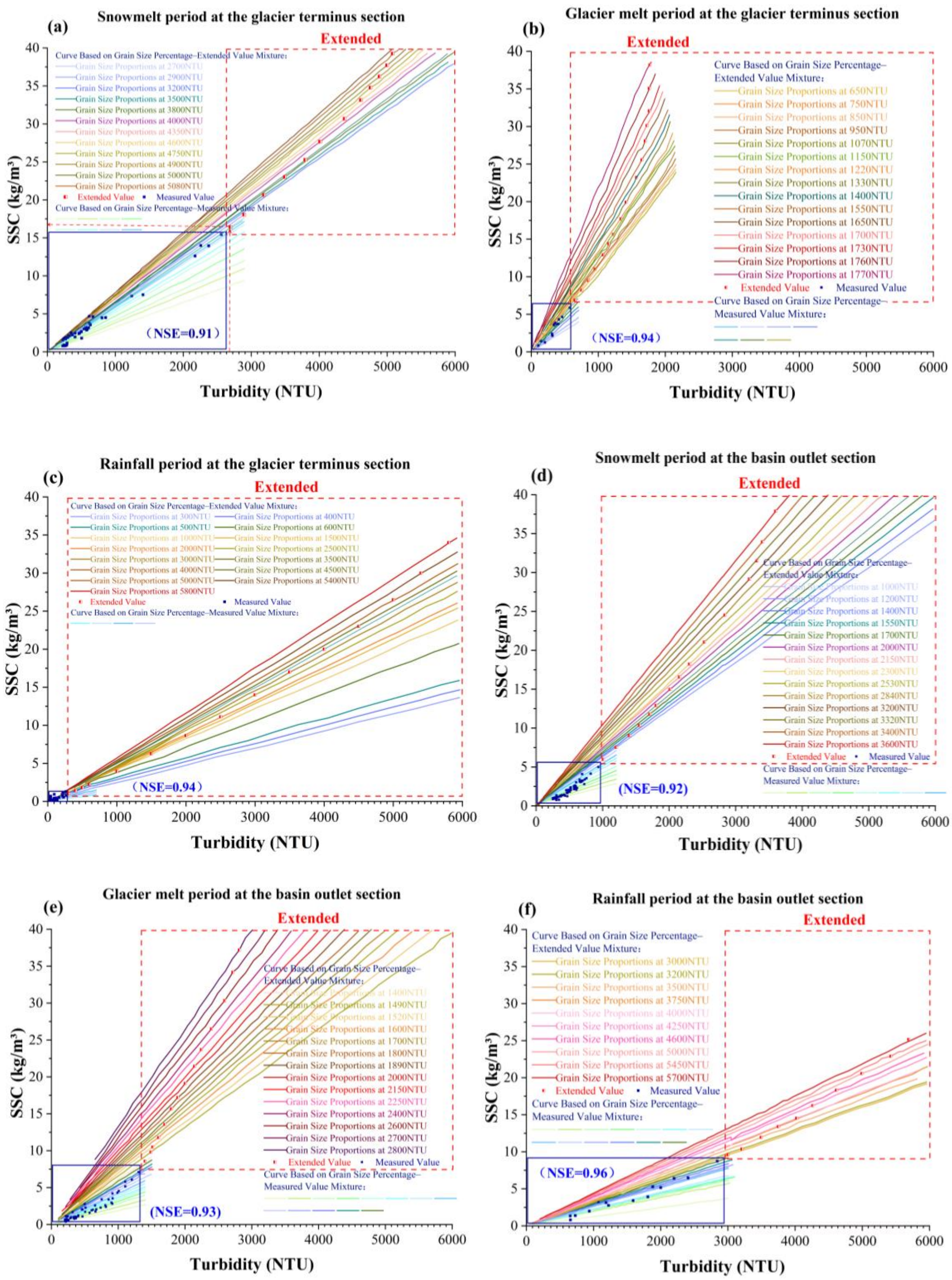

Fig. S13. Extension of the turbidity-SSC relationships.